



Italian Association of Aeronautics and Astronautics

XXII Conference

Napoli, 9-12 September 2013

## EFFECT OF LOADING FACTORS ON THE ANALYSIS OF AERONAUTICAL STRUCTURES BY COMPONENT-WISE MODELS

E. Carrera<sup>\*</sup>, F. Miglioretti, A. Pagani, F. Zangallo

Politecnico di Torino, Department of Mechanical and Aerospace Engineering, Corso Duca degli Abruzzi 24, 10129 Torino, Italy

\*erasmo.carrera@polito.it

### ABSTRACT

*The use of various finite elements (FE) for the analysis of reinforced-shell aerospace structures is discussed in this paper. One-, two-, and three-dimensional FE models from a commercial code are compared to higher-order beam theories, which are implemented by using the Carrera Unified Formulation (CUF). CUF is a hierarchical formulation allowing for the straightforward implementation of any order-beam theories without the need of ad-hoc formulations. The attention is here focused on a novel approach denoted as Component-Wise (CW). According to CUF, Lagrange-like polynomials are used in CW models to discretize the displacement field on the cross-section of each component of the structure. Depending on the geometrical and material characteristics of the component, the capabilities of the model can be enhanced and the computational costs can be kept low through smart discretization strategies. The global mathematical model of complex structures (e.g. wings or fuselages) is obtained by assembling each component model at the cross-section level. Next, a classical 1D FE formulation is used to develop numerical applications. A number of typical aerospace structures are analysed. Static and dynamic analyses highlight the enhanced capabilities of the proposed formulation. In fact, the CW approach is clearly the natural tool to analyse aerospace structures, since it leads to results that can be only obtained through three-dimensional elasticity (solid) elements whose computational costs are at least one-order of magnitude higher than CW models.*

**Keywords:** Aerospace structures; Beams; Unified Formulation; Component-wise

### 1 INTRODUCTION

Primary aircraft structures are essentially reinforced thin shells [1] and they are obtained by assembling three main components: skins, longitudinal stiffening members (including spar caps) and ribs. The free vibration analysis and the determination of stress/strain fields in these structural components are of prime interest for structural analysts. Many different approaches were developed in the first half of the last century. These are discussed in major reference books [1,2] and more recently in [3]. Due to the advent of computational methods, mostly FEM, the analysis of complex aircraft structures continued to be made using a combination of solids (3D), plates/shells (2D) and beams (1D). These were implemented first in NASTRAN codes. Many others commercial FE codes have been developed and used in aerospace

industries. Nowadays FEM models with a number of unknowns (degrees of freedom, DOFs) close to  $10^6$  are widely used in common practise. The possible manner in which stringers, spar caps, spar webs, panels, ribs are introduced into FE mathematical models is part of the knowledge of structural analysts. A short discussion of this follows. A number of works have shown the necessity for a proper simulation of the stiffeners-panel “linkage”. Kolli and Chandrashekhara [4] formulated an FE model with 9-node plate and 3-node beam elements. Gangadhara [5] carried out linear static analyses of composite laminated shells using a combination of 8-node plate elements and 3-node beam elements. In [6], Thin and Khoa developed a new 9-node rectangular stiffened plate element for the free vibration analysis of laminated stiffened plates based on Mindlin’s deformation plate theory. The works mentioned so far show a clear interest in investigating FEM applications to reinforced-shell structures. In most of the articles in literature, such as those cited above, plates/shells and stiffeners are modeled as separate elements and a simulation of the stiffener-panel “linkage” is often necessary. Usually, beam nodes are connected to the shell element nodes via rigid fictitious links. This methodology presents some inconsistencies.

The main aim of the present work is to introduce a new 1D formulation which is able to model reinforced-shell aircraft structures. The present component-wise (CW) approach deals with shells and stiffeners by means of a unique 1D formulation, with no need to introduce “fictitious links” to connect beam and shell elements. The CW approach has recently been exploited for the analysis of laminated composites [7] and it shown its enhanced capabilities in dealing with both static [8] and free vibration [9] analysis of wing structures. The present work is part of the framework of the one-dimensional Carrera Unified Formulation, CUF, which was recently proposed by the first author and his co-workers [10, 11]. Two classes of CUF 1D models were formulated: the Taylor-expansion class, hereafter referred to as TE, and the Lagrange-expansion class, hereafter referred to as LE. TE models exploit N-order Taylor-like polynomials to define the displacement field above the cross-section with N as a free parameter of the formulation [10,12]. An important feature of TE models is that Euler-Bernoulli (EBBM) and Timoshenko (TBM) classical beam theories can be derived as special cases of the linear Taylor-type expansion. Conversely, the LE class is based on Lagrange-like polynomials to discretize the cross-section displacement field and LE models have only pure displacement variables [11]. In the following a brief overview on CUF is proposed and the CW approach is described. Next, some examples are addresses. Finally, the main conclusions are outlined.

## 2 1D REFINED ELEMENTS

The adopted rectangular Cartesian coordinate system is shown in Figure 1, together with the geometry of the beam. The cross-sectional plane of the structure is denoted by " $\Omega$ " , and the beam boundaries over y are  $0 < y < L$ .

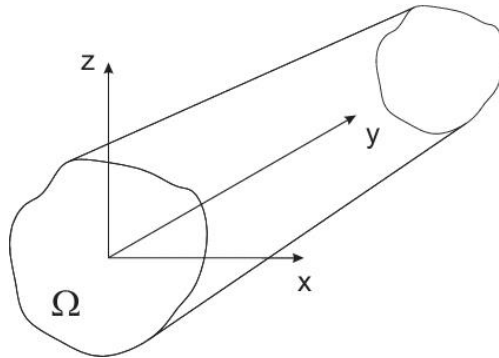


Figure 1: Coordinate frame of the beam model.

Let us introduce the transposed displacement vector,

$$\mathbf{u}(x, y, z) = \{u_x \ u_y \ u_z\}^T \quad (1)$$

Within the framework of the CUF, the displacement field can be expressed as

$$\mathbf{u}(x, y, z) = F_\tau(x, z)\mathbf{u}_\tau(y) \quad \tau = 1, 2, \dots, M \quad (2)$$

where  $F_\tau$  are the functions of the coordinates  $x$  and  $z$  on the cross-section.  $\mathbf{u}_\tau$  is the vector of the generalized displacements,  $M$  stands for the number of terms used in the expansion, and the repeated subscript,  $\tau$ , indicates summation. The choice of  $F_\tau$  determines the class of the 1D CUF model.

TE models consist of a Taylor series that uses the 2D polynomials  $x^i, z^j$  as base, where  $i$  and  $j$  are positive integers. For instance, the displacement field of the second-order ( $N = 2$ ) TE model can be expressed as

$$\begin{aligned} u_x &= u_{x_1} + xu_{x_2} + zu_{x_3} + x^2u_{x_4} + xzu_{x_5} + z^2u_{x_6} \\ u_y &= u_{y_1} + xu_{y_2} + zu_{y_3} + x^2u_{y_4} + xzu_{y_5} + z^2u_{y_6} \\ u_z &= u_{z_1} + xu_{z_2} + zu_{z_3} + x^2u_{z_4} + xzu_{z_5} + z^2u_{z_6} \end{aligned} \quad (3)$$

The order  $N$  of the expansion is set as an input option of the analysis. Classical TBM and EBBM theories are also captured from the formulation as degenerate cases of the linear ( $N = 1$ ) TE model. For LE class,  $F_\tau$  are Lagrange-like polynomials. In this work, three types of cross-section polynomial sets were adopted: four- (L3), four- (L4), and nine-point (L9) elements. The L3, L4 and L9 interpolation functions are given in [13]. Unlikely TE, one of the most important feature of LE models is that they have only pure displacement degrees of freedom. More details about LE models can be found in the paper by Carrera and Petrolo [11]. For both TE and LE models, the FE approach was adopted to discretize the structure along the  $y$ -axis. This process is conducted via a classical finite element technique, where the displacement vector is given by

$$\mathbf{u}(x, y, z) = F_\tau(x, z)N_i(y)\mathbf{q}_{\tau i} \quad (4)$$

$N_i$  stands for the shape functions and  $\mathbf{q}_{\tau i}$  for the nodal displacement vector. For the sake of brevity, the shape functions are not reported here. They can be found in many books, for instance in [13]. Elements with four nodes (B4) were adopted in this work, that is, a cubic approximation along the  $y$ -axis was assumed. The stiffness matrix of the elements, the external loadings vector and the mass matrix were obtained via the principle of virtual displacements

$$\delta L_{int} = \int_V \delta \boldsymbol{\varepsilon}^T \boldsymbol{\sigma} dV = \delta L_{ext} - \delta L_{ine} \quad (5)$$

where  $L_{int}$  stands for the strain energy,  $L_{ext}$  is the work of the external loadings and  $L_{ine}$  is the work of inertial loadings.  $\delta$  stands for the virtual variation.  $\boldsymbol{\varepsilon}$  and  $\boldsymbol{\sigma}$  are the vectors of the strains and stresses, respectively. For the sake of brevity, the derivation of the fundamental

nuclei is not reported here. They can be found in [8-11], together with a more comprehensive discussion on refined 1D CUF models.

## 2.1 The component-wise approach

The refined TE models described above are characterized by degrees of freedom (displacements and N-order derivatives of displacements) with a correspondence to the axis of the beam. The expansion can also be made by using only pure displacement values, e.g. by using Lagrange polynomials. The resulting LE can be used for the whole cross-section or can be introduced by dividing the cross-section into various sub-domains (see [11]). This characteristic allows us to separately model, for instance, stringers and panels. The LE formulation was used in this paper to implement CW models of reinforced-shell wing structures, as shown in Figure 2a where a two-stringer spar is considered. Figure 2b shows

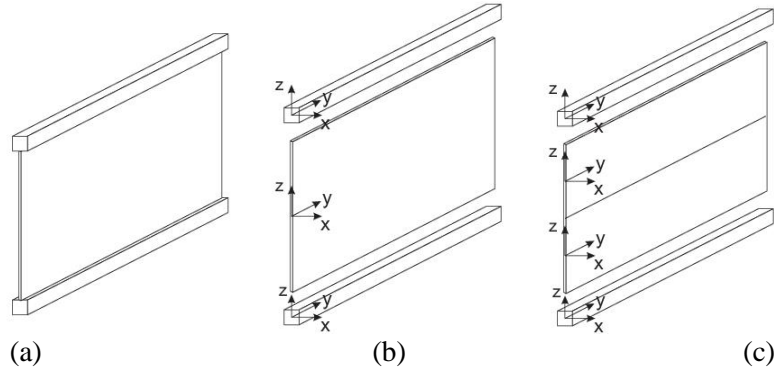


Figure 2: CW approach through LE elements

a possible CW model of the spar where each component was modelled via one 1D LE element. Each LE element is then assembled above the cross-section to obtain the global stiffness matrix based on the 1D formulation. Since panels could not be reasonably modelled via a 1D formulation, 1D CW models can be refined by using several L-elements for one component. This aspect is shown in Figure 2c where the panel is modelled via two 1D LE elements. By exploiting the present 1D formulation, the analysis capabilities of a structural model can be enhanced by 1. locally refining the LE discretization; 2. using higher-order LE elements (e.g. 4-node, 9-node, etc.).

## 3 NUMERICAL RESULTS

The efficiency of both CW and TE refined models is investigated in this section. First, the results from the modal analysis of a C-shaped beam are given in order to highlight the main capabilities of the present methods. The results from static analysis of a complex wing structure are subsequently introduced. Comparisons with MSC Nastran 3D solid models are proposed. Particular attention is given to the capabilities offered by CW models of dealing with complex thin-walled reinforced structures as well as with solid -like FEM analyses with significantly lower computational costs.

### 3.1 Free vibration analysis of a C-shaped beam

A cantilever C-shaped beam is considered as the first numerical example. The cross-section of the structure is shown in Figure 3. The geometrical data are as follows:  $b_2 = h = 1$  m,  $b_1 = 0.5$  m,  $t = 0.1$  m. The length of the beam  $L$  is equal to 20 m. The structure is made of an aluminium alloy with Young's modulus  $E = 75$  GPa, Poisson's ratio  $\nu = 0.33$ , and density  $\rho = 2700$  Kg/m<sup>3</sup>.

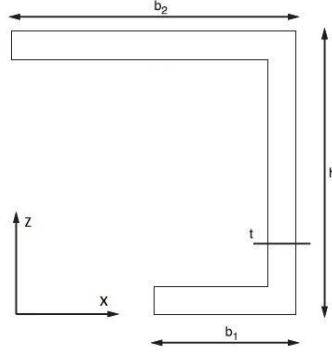


Figure 3: Cross-section of the C-shaped beam

Table 1 shows the first ten natural frequencies according to classical, refined, component-wise, and a Nastran solid models. The given results refer to a configuration in which a *non-structural mass* is placed at  $(0, h, L)$ . Columns 2 and 3 show the results by classical beam theories. Columns 4 to 7 show the natural frequencies by fourth- to eight-order TE model. In columns 8 and 9 the results by CW models of the C-shaped beam are given. Two CW models are considered, differing in the L-element discretization of the cross-section, as shown in Figure 4, where the location of the non-structural mass is also depicted. Specifically, the 6L9 model is built with six nine-node Lagrange elements on the cross-section, whereas the 10L9 model is composed by 10 nine-node L-elements. In the last column the results of a solid model by MSC Nastran are also given for comparison purposes. In Table 1, the number of the degrees of freedom (DOFs) is also given for each model implemented.

	EBBM	TBM	N=2	N=4	N=6	N=8	6L9	10L9	Solid
DOFs	93	155	558	1395	2604	4185	3627	5859	177000
1	1.154 <sup>f</sup>	1.153 <sup>f</sup>	1.158 <sup>f</sup>	1.152 <sup>f</sup>	1.137 <sup>ft</sup>	1.126 <sup>ft</sup>	1.115 <sup>ft</sup>	1.115 <sup>ft</sup>	1.111 <sup>ft</sup>
2	1.971 <sup>f</sup>	1.967 <sup>f</sup>	1.973 <sup>f</sup>	1.895 <sup>f</sup>	1.736 <sup>ft</sup>	1.651 <sup>ft</sup>	1.589 <sup>ft</sup>	1.586 <sup>ft</sup>	1.579 <sup>ft</sup>
3	8.675 <sup>f</sup>	8.630 <sup>f</sup>	8.576 <sup>f</sup>	7.628 <sup>f</sup>	5.705 <sup>t</sup>	5.168 <sup>t</sup>	4.901 <sup>t</sup>	4.889 <sup>t</sup>	4.560 <sup>t</sup>
4	14.699 <sup>f</sup>	14.486 <sup>f</sup>	14.356 <sup>t</sup>	11.371 <sup>t</sup>	9.283 <sup>t</sup>	8.375 <sup>t</sup>	7.771 <sup>t</sup>	7.734 <sup>t</sup>	7.670 <sup>t</sup>
5	25.765 <sup>f</sup>	25.444 <sup>f</sup>	23.585 <sup>ft</sup>	12.603 <sup>ft</sup>	10.096 <sup>ft</sup>	9.823 <sup>ft</sup>	9.735 <sup>ft</sup>	9.728 <sup>ft</sup>	9.862 <sup>ft</sup>
6	41.504 <sup>f</sup>	40.489 <sup>f</sup>	30.962 <sup>ft</sup>	25.286 <sup>ft</sup>	20.642 <sup>ft</sup>	18.238 <sup>ft</sup>	16.920 <sup>ft</sup>	16.810 <sup>ft</sup>	16.633 <sup>ft</sup>
7	49.009 <sup>f</sup>	48.075 <sup>f</sup>	41.005 <sup>ft</sup>	30.465 <sup>ft</sup>	23.374 <sup>ft</sup>	22.831 <sup>ft</sup>	22.718 <sup>ft</sup>	22.643 <sup>ft</sup>	22.235 <sup>ft</sup>
8	54.789 <sup>f</sup>	53.782 <sup>f</sup>	48.724 <sup>ft</sup>	35.776 <sup>ft</sup>	29.792 <sup>ft</sup>	28.698 <sup>ft</sup>	27.426 <sup>ft</sup>	27.169 <sup>ft</sup>	26.716 <sup>ft</sup>
9	85.837 <sup>f</sup>	81.860 <sup>f</sup>	54.363 <sup>ft</sup>	42.934 <sup>ft</sup>	33.487 <sup>ft</sup>	30.518 <sup>ft</sup>	29.704 <sup>ft</sup>	29.647 <sup>ft</sup>	29.514 <sup>ft</sup>
10	89.333 <sup>f</sup>	85.371 <sup>f</sup>	79.443 <sup>ft</sup>	51.675 <sup>ft</sup>	40.656 <sup>ft</sup>	38.247 <sup>ft</sup>	39.120 <sup>ft</sup>	38.162 <sup>ft</sup>	34.359 <sup>ft</sup>

\*f: flexural mode, t: torsional mode; ft: coupled mode

Table 1: Natural frequencies of the C-shaped beam. f: flexural mode, t: torsional mode, ft: coupled mode.

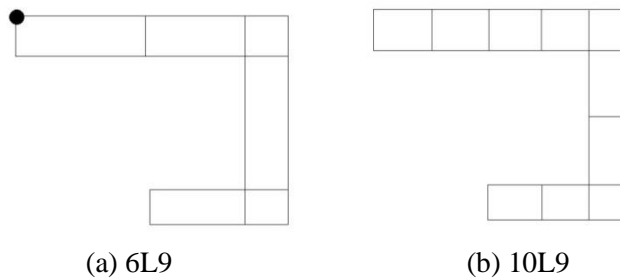


Figure 4: CW models of the C-shaped beam

From the analysis it is clear that both TE and CW models are able to deal with solid-like results with very low computational efforts. In particular, it has been demonstrated that higher-than-sixth-order TE beam models are necessary to correctly describe torsional behaviours. Moreover, it is shown that higher-order TE and CW models can detect non local effects due to non-localized non-structural masses.

### 3.2 Static response of a complete wing structure

A more complex aeronautical structure is considered as the second assessment. The wing which is shown in Figure 5, consists of a NACA 2415 airfoil with two spars. The dimensions of the section are shown in Figure 5. The wing has a chord  $c$  - constant along the length - equal to 1 m. The wing half-span, i.e. the length of the beam  $L$ , is 6 m. The whole structure is made of the same material as in the previous example and clamped-free boundary conditions are considered. The structure undergo an inertial load  $n = 1$  g in the negative direction of the  $z$ -axis.

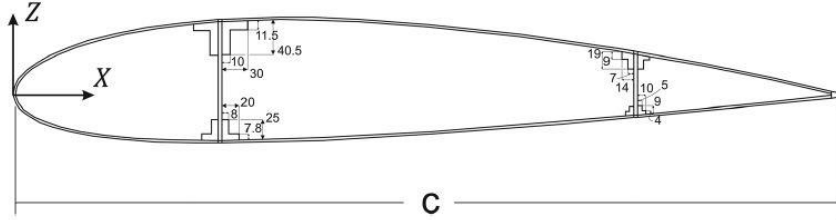


Figure 5: Cross-section of the wing structure. Dimensions in millimetres.

In Table 2 the maximum values of the vertical displacement are given for each model implemented. Both classical and higher-order models are considered in Table 2. A solid model by MSC Nastran is also considered for comparisons. The number of DOFs are also given in Table 2.

Model	$-u_z$ , cm	DOFs
Classical Beam theories		
EBBM	2.147	84
TBM	2.149	140
TE models		
N=2	2.075	504
N=4	2.101	1260
N=6	2.109	2352
N=7	2.112	3024
N=8	2.113	3780
N=9	2.115	4620
CW model		
49L9	2.123	24864
MSC Nastran model		
Solid	2.143	186921

Table 2: Maximum value of the vertical displacement, wing structure

Figure 6 shows the normal stress distribution,  $\sigma_{yy}$ , in the top left stringer at  $x = 0.25$  m,  $z = 0.057$  m versus  $y$ -axis. Figure 7 shows the distribution along the  $z$ -axis of transverse shear stress,  $\sigma_{yz}$ , in the front spar at  $y = 2$  m. The results by the component-wise and higher-order TE models are compared with the solution from the Solid model by MSC Nastran.

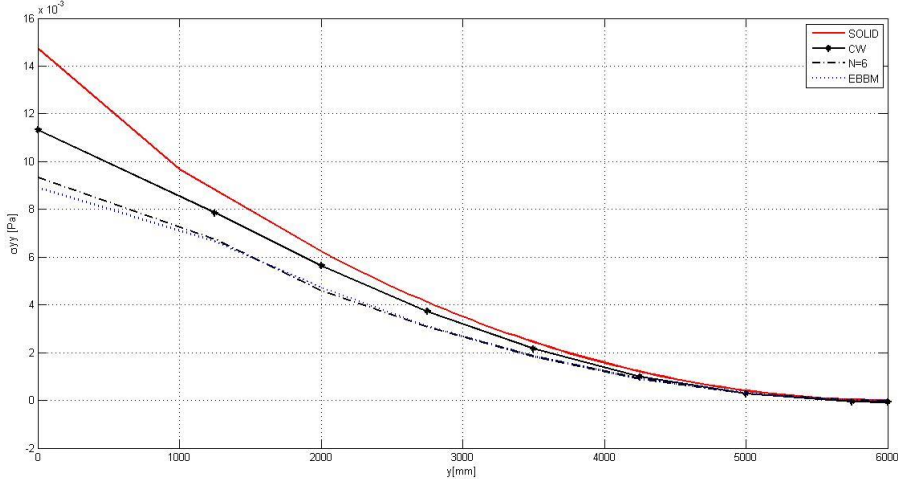


Figure 6: Span-wise distribution of the axial stress component,  $\sigma_{yy}$ , in the top left stringer ( $x = 0.25$  m,  $z = 0.057$  m).

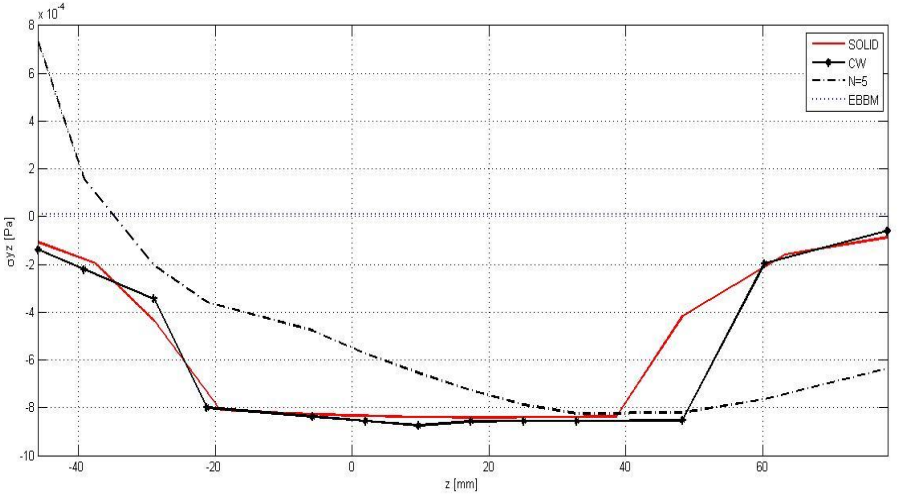


Figure 7: Distribution of the shear stress component,  $\sigma_{yz}$ , in the front spar at  $y = 2$  m.

The results point out that CW results are in good agreement with solid FEM solution, both in terms of displacement and stress distributions. Conversely, classical and higher-order TE models are not able to correctly describe the stress state of the structure under consideration.

#### 4 CONCLUSIONS

A Component-wise approach has been introduced in this paper by using the Carrera Unified Formulation. Numerical results have been produced and aeronautical structures considered. The results have been compared to classical and refined beam theories, as well as to 3D solid models from the commercial code MSC Nastran. The main conclusion to be drawn is that the present component-wise analysis appears to the authors to be the most convenient way, in

terms of both accuracy and computational costs, to capture the mechanical behaviour of aircraft structures.

## REFERENCES

- [1] E.F. Bruhn. *Analysis and Design of Flight Vehicle Structures*. Tri-State Offset Company, Cincinnati, USA (1973).
- [2] R.M. Rivello. *Theory and Analysis of Flight Structures*. McGraw-Hill, New York, USA (1969).
- [3] E. Carrera. *Fondamenti sul Calcolo di Strutture a Guscio Rinforzato per Veicoli Aero-spaziali*. Levrotto & Bella, Torino, Italy (2011).
- [4] M. Kolli, K. Chandrashekhara. Finite element analysis of stiffened laminated plates under transverse loading. *Composite Science and Technology*, **56**, pp. 1355-1361 (1996).
- [5] B.P. Gangadhara. Linear static analysis of hat stiffened laminated shells using finite elements. *Finite Elements in Analysis and Design*, **39**, pp. 1125-1138 (2003).
- [6] T.I. Thinh, N.N. Khoa. Free vibration analysis of stiffened laminated plates using a new stiffened element. *Technische Mechanik*, **28**(3-4), pp. 227-236 (2008).
- [7] E. Carrera, M. Maiarù, M. Petrolo. Component-wise analysis of laminated anisotropic composites. *International Journal of Solids and Structures*, **49**, pp. 1839-1851 (2012).
- [8] E. Carrera, A. Pagani, M. Petrolo. Classical, refined and component-wise theories for static analysis of reinforced-shell wing structures. *AIAA Journal*, **51**(5), pp. 1255-1268 (2013).
- [9] E. Carrera, A. Pagani, M. Petrolo. Component-wise method applied to vibration of wing structures. *Journal of Applied Mechanics*, **8**(4), pp. 041012/1-041012/15 (2013).
- [10] E. Carrera, G. Giunta, M. Petrolo. *Beam Structures: Classical and Advanced Theories*. John Wiley & Sons (2011).
- [11] E. Carrera, M. Petrolo. Refined beam elements with only displacement variables and plate/shell capabilities. *Meccanica*, **47**(3), pp. 537-556 (2012).
- [12] E. Carrera, M. Petrolo, E. Zappino. Performance of CUF approach to analyze the structural behavior of slender bodies. *Journal of Structural Engineering*, **138**(2), pp. 285-297 (2012).
- [13] E. Ònate. *Structural Analysis with the Finite Element Method: Linear Statics, Volume 1*. Springer (2009).